



Numerical Study of Zakharov–Kuznetsov Equations in Two Dimensions

Christian Klein¹ · Svetlana Roudenko² · Nikola Stoilov¹

Received: 18 February 2020 / Accepted: 23 January 2021 / Published online: 15 February 2021
© The Author(s), under exclusive licence to Springer Science+Business Media, LLC part of Springer Nature 2021

Abstract

We present a detailed numerical study of solutions to the (generalized) Zakharov–Kuznetsov equation in two spatial dimensions with various power nonlinearities. In the L^2 -subcritical case, numerical evidence is presented for the stability of solitons and the soliton resolution for generic initial data. In the L^2 -critical and supercritical cases, solitons appear to be unstable against both dispersion and blow-up. It is conjectured that blow-up happens in finite time and that blow-up solutions have some resemblance of being self-similar, i.e., the blow-up core forms a rightward moving self-similar type rescaled profile with the blow-up happening at infinity in the critical case and at a finite location in the supercritical case. In the L^2 -critical case, the blow-up appears to be similar to the one in the L^2 -critical generalized Korteweg–de Vries equation with the profile being a dynamically rescaled soliton.

Keywords Zakharov–Kuznetsov equation · Solitons · Stability · Blow-up dynamics

Mathematics Subject Classification Primary 35Q53 · 37K40 · 37K45

Communicated by David Nicholls.

✉ Christian Klein
Christian.Klein@u-bourgogne.fr

Svetlana Roudenko
sroudenko@fiu.edu

Nikola Stoilov
Nikola.Stoilov@u-bourgogne.fr

¹ Institut de Mathématiques de Bourgogne, UMR 5584, Université de Bourgogne-Franche-Comté, 9 avenue Alain Savary, 21078 Dijon Cedex, France

² Department of Mathematics and Statistics, Florida International University, Miami, FL 33199, USA

1 Introduction

We are interested in the 2D generalized Zakharov–Kuznetsov (ZK) equation

$$u_t + (u_{xx} + u_{yy} + u^p)_x = 0, \quad p = 2, 3, 4. \tag{1}$$

This equation is a two-dimensional generalization of the well-known Korteweg–de Vries (KdV) equation, which is spatially limited as the 1D model of weakly nonlinear waves in shallow water. The 2D quadratic ($p = 2$) ZK equation governs, for example, weakly nonlinear ion-acoustic waves in a plasma comprising cold ions and hot isothermal electrons in the presence of a uniform magnetic field (Monro and Parkes 1999). In Melkonian and Maslowe (1989), this equation appears as the amplitude equation for two-dimensional long waves on the free surface of a thin film flowing down a vertical plane with moderate values of the fluid surface tension and large viscosity. While originally the equation was proposed by Zakharov and Kuznetsov in the 3D setting, see Zakharov and Kuznetsov (1974), the first rigorous derivation was done in Lannes et al. (2013) from the Euler–Poisson system. In this paper, we initiate numerical investigations of the two-dimensional ZK equation with pure power nonlinearities $p = 2, 3, 4$.

The well-posedness theory for the Cauchy problem for the ZK equation with H^1 initial data was initiated in Faminskii (1995), followed by lower regularity improvements in Linares and Pastor (2009), Farah et al. (2012) Ribaud and Vento (2012) and Kinoshita (2018). From the local theory, it follows that solutions to the ZK equation have a maximal forward lifespan $[0, T)$ with either $T = +\infty$ or $T < +\infty$. In the later case in the 2D setting, one has $\|\nabla u(t)\|_{L^2(\mathbb{R}^2)} \nearrow \infty$ as $t \rightarrow T$, though the unbounded growth of the gradient might also happen in infinite time.

During their existence, solutions to ZK have several conserved quantities, relevant to this work is the L^2 norm (or mass), and the energy (or Hamiltonian):

$$\begin{aligned} M[u(t)] &= \int_{\mathbb{R}^2} u^2(t) = M[u(0)], \\ E[u(t)] &= \frac{1}{2} \int_{\mathbb{R}^2} (u_x^2(t) + u_y^2(t)) - \frac{1}{p+1} \int_{\mathbb{R}^2} u^{p+1}(t) = E[u(0)]. \end{aligned} \tag{2}$$

Unlike the 1D KdV or modified KdV, the ZK equation is not integrable for any power p .

One of the useful symmetries in the evolution equations is *the scaling invariance*, which states that an appropriately rescaled version of the original solution is also a solution of the equation. For Eq. (1), it is

$$u_\lambda(x, y, t) = \lambda^{\frac{2}{p-1}} u(\lambda x, \lambda y, \lambda^3 t). \tag{3}$$

This symmetry makes invariant the Sobolev norm \dot{H}^s with $s = 1 - \frac{2}{p-1}$, since $\|u_\lambda\|_{\dot{H}^s} = \lambda^{\frac{2}{p-1} + s - 1} \|u\|_{\dot{H}^s}$. Moreover, the index s gives rise to the critical-type classification of (1): when $s < 0$, or $p < 3$, Eq. (1) is called the L^2 -subcritical equation

(in this paper a representative of this case is $p = 2$); if $p > 3$, or $s > 0$, the equation is L^2 -supercritical (we use $p = 4$), and with $p = 3$, or $s = 0$, it is L^2 -critical. This classification is important when one studies long time behavior of solutions for various nonlinearities. For that, we need the notion of solitons.

The 2D ZK equation has a family of localized traveling waves (or solitary waves, often referred to as solitons), which travel only in x -direction

$$u(x, y, t) = Q(x - ct, y) \tag{4}$$

satisfying

$$-cQ + Q_{xx} + Q_{yy} + Q^p = 0; \tag{5}$$

and defining the ground state solution (i.e., the unique radial positive H^1 solution vanishing at infinity, for which the existence, uniqueness and various other properties are well known, see, for example, Sulem and Sulem (1999)). We note that $Q \in C^\infty(\mathbb{R}^2)$, $\partial_r Q(r) < 0$ for any $r = |(x, y)| > 0$ and that Q has exponential decay $|\partial^\alpha Q(x, y)| \leq c_\alpha e^{-r}$ for any multi-index α and any $(x, y) \in \mathbb{R}^2$. The solitons $Q_c(x, y)$ are related to the soliton $Q_1(x, y) =: Q(x, y)$ for $c > 0$ via

$$Q_c(x, y) = c^{\frac{1}{p-1}} Q(\sqrt{c}x, \sqrt{c}y); \tag{6}$$

thus, it suffices to consider $c = 1$.

In the L^2 -subcritical case, the local theory together with the Gagliardo–Nirenberg inequality implies that the H^1 norm of solutions remains bounded, and thus, all solutions in the subcritical case exist globally in time. In the L^2 -critical case, using the energy and mass conservation together with the Gagliardo–Nirenberg inequality and its sharp constant expressed in terms of the soliton mass, one has $\|\nabla u\|_{L^2}^2 \leq (1 - \frac{\|u\|_{L^2}^2}{\|Q\|_{L^2}^2})^{-1} E[u]$. Thus, if $\|u_0\|_{L^2} < \|Q\|_{L^2}$, then solutions with the initial condition u_0 exist also globally in time, while the blow-up might be possible if the initial mass $\|u_0\|_{L^2}^2$ is greater or equal to that of the soliton Q .

The main aim of this work is to investigate behavior of solutions in various cases of the 2D ZK equation numerically. In particular, we are interested in stability of solitons and in their interaction in the subcritical case, in the scattering and blow-up behavior in the critical and supercritical cases. For that, we mention that the orbital stability of solitons in the context of the generalized ZK Eq. (1) was obtained by de Bouard (1996) showing that the traveling waves are orbitally stable in the 2D case for $p < 3$ and unstable for $p > 3$. The instability of solitons in the critical case $p = 3$ was shown by the second author and her collaborators in Farah et al. (2019), see also Farah et al. (2019) for an alternative proof of instability in the supercritical ZK case. The more refined asymptotic stability was obtained for $p = 2$ by Cote, Muñoz, Pilod and Simpson in Côte et al. (2016) (in fact, for $2 \leq p < p^* \approx 2.15$); in that work the authors also studied the interaction of N well-separated solitons (see also a recent result in Valet (2020)). The instability of solitons in the critical ($p = 3$) case led to showing the existence of blow-up in the 2D critical ZK equation. The first such rigorous work in a higher dimensional generalization of generalized KdV (gKdV) equation is (Farah

et al. 2018) (for prior work indicating a possibility of collapse in the 2D modified ZK, see Sipcic and Benney (2000)). In Farah et al. (2018), the blow-up is shown for initial data with negative energy and the mass slightly above the ground state mass. We note that unlike other dispersive equations such as the nonlinear Schrödinger equation (NLS), the KdV-type equations (including ZK equation) do not have a convenient virial identity, which gives a straightforward proof of existence of blow-up solutions. Therefore, the proof of existence of blow-up solutions via analytical tools has only been done via construction of such solutions, for example, for the blow-up in 1D critical gKdV see Merle (2001) and Martel and Merle (2002).

In this paper, we investigate the following conjectures about the stability of solitons in the L^2 -subcritical case, about scattering and the stable blow-up dynamics in the L^2 -critical and supercritical cases.¹

Conjecture 1 (L^2 -subcritical case). *Consider the subcritical 2D ZK equation, in particular, when $p = 2$ in (1).*

- (1) *The soliton solutions (4)–(5)–(6) are orbitally and asymptotically stable.*
- (2) *Solutions of (1) with general sufficiently localized initial data and of sufficient smoothness decompose as $t \rightarrow \infty$ into solitons and radiation.*

Conjecture 2 (L^2 -critical case). *Consider the critical 2D ZK Eq. (1) with $p = 3$.*

- (1) *If $u_0 \in \mathcal{S}(\mathbb{R}^2)$ is such that $\|u_0\|_2 < \|Q\|_2$, then the solution $u(t)$ to (1) is dispersed.*
- (2) *If $u_0 \in \mathcal{S}(\mathbb{R}^2)$ is sufficiently localized and such that $\|u_0\|_2 > \|Q\|_2$, then the solution blows up in finite time $t = t^*$ and such that as $t \rightarrow t^*$*

$$u(x, y, t) - \frac{1}{L(t)} Q\left(\frac{x - x_m(t)}{L(t)}, \frac{y - y_m(t)}{L(t)}\right) \rightarrow \tilde{u} \in L^2, \tag{7}$$

with

$$\|u_x(t)\|_2 \sim \frac{1}{L(t)}, \quad L(t) \sim \sqrt{t^* - t}, \quad \text{and} \quad x_m(t) \sim \frac{1}{t^* - t}, \quad y_m(t) \rightarrow y^* < \infty. \tag{8}$$

Conjecture 3 (L^2 -supercritical case). *Consider the supercritical 2D ZK equation, in particular, when $p = 4$ in (1). Let $u_0 \in \mathcal{S}(\mathbb{R}^2)$ be of sufficiently large mass and energy² and of some localization. Then, ZK evolution $u(t)$ blows up in finite time t^* and finite location (x^*, y^*) , i.e., the blow-up core resembles a self-similar structure with*

$$u(x, y, t) - \frac{1}{L^{\frac{2}{p-1}}(t)} P\left(\frac{x - x_m(t)}{L(t)}, \frac{y - y_m(t)}{L(t)}\right) \rightarrow \tilde{u} \in L^2, \tag{9}$$

where $P(x, y)$ is a localized solution to (18) (which is conjectured to exist),

$$x_m(t) \rightarrow x^*, \quad y_m(t) \rightarrow y^*,$$

¹ In our conjectures and simulations, we consider exponentially decaying initial data; it will be interesting to investigate slower decay conditions.

² We have not investigated numerically the precise value. For some thresholds, for example, see Farah et al. (2012).

and

$$\|u_x(t)\|_2 \sim \frac{1}{L^{\frac{2}{p-1}}(t)} \quad \text{with } L(t) \sim (t^* - t)^{1/3} \quad \text{as } t \rightarrow t^*. \quad (10)$$

Remark 1.1 We note that numerical blow-up computations are extremely challenging, since they push the limits of the best currently available methods, approaches and computational power. This is especially true for dispersive equations, where also the radiation should be correctly approximated. In a sense, this can be seen as an invitation to analytical studies of the phenomena shown in this paper (see some work in this direction (Farah et al. 2018, 2019; Côte et al. 2016)). Nonetheless, the techniques applied here have been successfully tested on an example of the gKdV equation, for which the analytical description is much better understood, though far from being complete.

The paper is organized as follows: In Sect. 2, we present the numerical tools used to solve the ZK equation. Examples for the L^2 -subcritical case are discussed in Sect. 3. The L^2 -critical case is studied in Sect. 4. In Sect. 5, we discuss examples for the L^2 -supercritical case.

2 Numerical Methods

In this section, we review the numerical methods to be applied in the rest of the paper. First, we construct the ZK solitons via an iterative approach. Then, we introduce the integration of the ZK equation with a Fourier spectral method for the spatial coordinates and a fourth-order scheme in time. Finally, we review the dynamic rescaling method, which is used to track blow-up solutions.

2.1 Solitons

We first obtain the soliton solutions for Eq. (1) by solving Eq. (5). Since this is also the defining equation for the solitons of the NLS equation in 2D, it is known that its solutions have radial symmetry. Here, we do not use this fact, since we intend to apply Fourier methods throughout the paper and thus directly construct the solitons on the grids for the time evolution.

To this end, we use discrete Fourier transforms in both x and y , which is, loosely speaking, equivalent to approximating a function via a truncated Fourier series. Since it is known that the NLS solitons are rapidly decreasing functions, they can be treated as periodic smooth functions on sufficiently large periods within the finite numerical precision. We work with $x \in L_x[-\pi, \pi]$ and $y \in L_y[-\pi, \pi]$, where L_x and L_y are positive real numbers, chosen so that the Fourier coefficients decrease both in x and y to machine precision (which is of the order of 10^{-16} in double precision). We denote the dual Fourier variables to x and y by k_x and k_y , respectively, and write

$$Q(x, y) \approx \sum_{k_x=-N_x/2+1}^{N_x/2} \sum_{k_y=-N_y/2+1}^{N_y/2} \hat{Q}(k_x, k_y) e^{i(k_x x + k_y y)}; \quad (11)$$

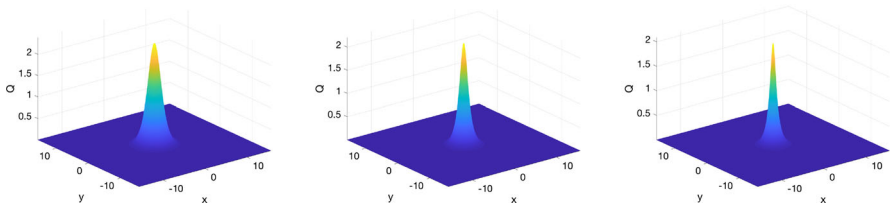


Fig. 1 Solitons to ZK Eq. (5) for $c = 1$ and $p = 2, 3, 4$ from left to right

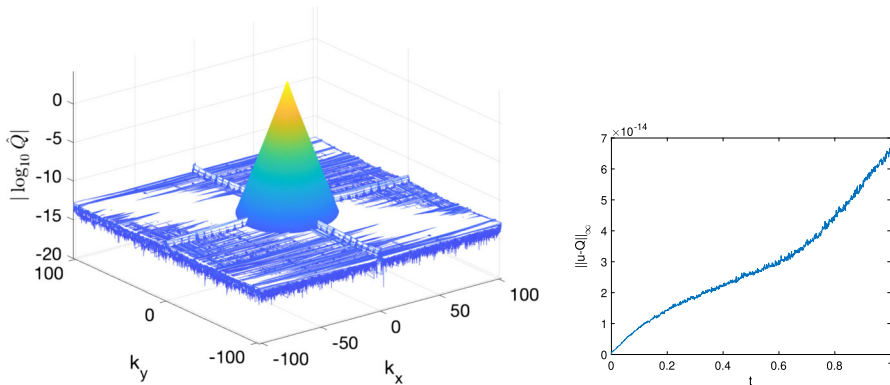


Fig. 2 Left: Modulus of the Fourier coefficients of the ZK soliton with $c = 1$ and $p = 3$. Right: the difference between the numerically computed solution to (1) with $p = 3$ with the soliton initial condition and the soliton from (5), depending on time

the discrete Fourier transform $\hat{Q} = \mathcal{F}u$ can be conveniently computed with a fast Fourier transform (FFT). An advantage of Fourier methods is that the numerical resolution can be controlled via the decay of the Fourier coefficients; the highest coefficients indicate the numerical error introduced by the truncation of the series.

With this Fourier discretization, Eq. (5) is approximated by an $N_x N_y$ dimensional system of nonlinear equations for the \hat{Q} . The latter will be iteratively solved by a Newton-Krylov iteration. This means that we invert the Jacobian via Krylov subspace methods as in Arbunich et al. (2019), here GMRES (Saad and Schultz 1986). We use $N_x = N_y = 2^{10}$, $L_x = L_y = 10$ and $Q = 2 e^{-x^2-y^2}$ as initial iterates in all cases. The iteration is stopped when the residual is smaller than 10^{-10} . The solitons for $c = 1$ and $p = 2, 3, 4$ are shown in Fig. 1. It can be seen that they become more localized and slightly smaller with increasing nonlinearity (the maximum value, which is also the value at zero, decreases: $Q(0) = 2.3920$ if $p = 2$, $Q(0) = 2.2062$ if $p = 3$, and $Q(0) = 2.0853$ if $p = 4$). The Fourier coefficients decrease in all cases to machine precision, see Fig. 2 on the left for $p = 3$, which implies that the solution is spatially well resolved.

2.2 Time Evolution

The same Fourier discretization as for the soliton above is used for the full ZK Eq. (1), which is thus approximated by an $N_x N_y$ dimensional system of ordinary differential

equations in t of the form

$$\hat{u}_t = \mathcal{L}\hat{u} + \mathcal{N}[\hat{u}], \tag{12}$$

where $\mathcal{L} = ik_x(k_x^2 + k_y^2)$ and $\mathcal{N}[\hat{u}] = -ik_x\mathcal{F}(u^p)$. Because of the appearance of third derivatives in x and y , this system is *stiff*, implying that explicit methods will be inefficient due to stability conditions as they necessitate prohibitively small time steps in order to stabilize the code. Implicit schemes are less restrictive in this sense, but are computationally expensive, since the resulting nonlinear equation has to be solved in each time step. Therefore, we have compared in Klein (2008) and Klein and Roidot (2011) various adapted integrators for stiff systems with a diagonal \mathcal{L} as we have here, which are explicit and of fourth order. It turned out that *exponential time differencing* (ETD) schemes, see Hochbruck and Ostermann (2010) for a comprehensive review with many references, are most efficient in the context of KdV-type equations. There are various fourth order ETD methods, which all showed a similar performance in our tests. Here, we apply the method in Cox and Matthews (2002) in the implementation described in Klein (2008) and Klein and Roidot (2011). The accuracy of the time integration scheme can be controlled via the conserved energy of the equation. Due to limitations in the accuracy of numerical methods, the computed energy (again Fourier techniques are applied to (2)) will not be exactly conserved. The quantity $\Delta E = |E(t)/E(0) - 1|$ can be used as discussed in Klein (2008) and Klein and Roidot (2011) as an estimate of the numerical error. Typically, it overestimates the accuracy of the numerical solution by 1–2 orders of magnitude.

As far as the blow-up is concerned, it is numerically very challenging to study blow-up solutions. For the generalized KdV and KP equations, this was done, for instance, in Klein and Peter (2014) and Klein and Peter (2015). There it was shown that the integration of the dynamically rescaled Eq. (16) is problematic if Fourier methods are used. Instead in Klein and Peter (2014), Klein and Peter (2015) and Klein and Stoilov (2018), the equations were integrated without rescaling, and then, a post-processing of the results was done according to (15) to identify the type of the blow-up. The same strategy will be applied here to ZK. However, the generalized KdV equations have the additional complication that the blow-up occurs at infinite values of x and that the blow-up profile is leaving the initial location with infinite velocity. To treat such cases, in Klein and Peter (2014) and Arbunich et al. (2019) we introduced a reference frame, in which the maximum of the solution is stationary at some point x_m during the whole computation, i.e., an accelerated reference frame. This means we apply (15) with $L = 1$ and $y_m = 0$ and solve

$$u_t + (u_{xx} + u_{yy} + u^p)_x - v_x u_x = 0, \quad p = 2, 3, 4, \tag{13}$$

where $u(x_m)$ is taken to be a maximum of the solution for all times. By differentiating Eq. (13) with respect to x and evaluating it for $x = x_m$, we get

$$v_x = \frac{(u_{xx} + u_{yy} + u^p)_{xx}}{u_{xx}} \Big|_{x=x_m}. \tag{14}$$

Since it is computationally expensive to compute v_x in each time step, we only apply this approach for blow-up computations in the L^2 critical case.

2.3 Test

To test the time evolution code and the soliton at the same time, we consider the soliton in the L^2 -critical case ($p = 3$) as initial data and a co-moving frame with $v_x = c = 1$. For $t \in [0, 1]$, we apply $N_t = 1000$ time steps. The numerically computed energy is conserved to the order of 10^{-14} . The difference between the numerically computed solution and the soliton can be seen on the right of Fig. 2. It increases with time, but is of the order of 10^{-14} as the energy conservation. Though we show later that the soliton is unstable against both dispersion and blow-up, the code is able to propagate it on the considered time intervals with essentially machine precision.

2.4 Dynamic Rescaling

Recalling the scaling invariance (3) for Eq. (1), one can use this symmetry in the context of blow-up in the form of a *dynamical rescaling*

$$X = \frac{x-x_m(t)}{L(t)}, \quad Y = \frac{y-y_m(t)}{L(t)}, \quad T = \int_0^t \frac{dt'}{L^3(t')},$$

$$U(X, Y, T) = L^{\frac{2}{p-1}}(t) u(x, y, t). \tag{15}$$

The dynamically rescaled ZK equation reads

$$U_T - a \left(\frac{2}{p-1} U + XU_X + YU_Y \right) - v_X U_X - v_Y U_Y + \left(U_{XX} + U_{YY} + U^p \right)_X = 0, \tag{16}$$

where

$$a \equiv a(T) = \frac{d \ln L}{dT}, \quad v_X = \frac{x_{m,T}}{L}, \quad v_Y = \frac{y_{m,T}}{L}. \tag{17}$$

It is assumed that blow-up happens as $T \rightarrow \infty$ and that U_T vanishes in this limit. Thus, Eq. (16) in the limit becomes

$$-\tilde{a} \left(\frac{2}{p-1} \tilde{U} + X\tilde{U}_X + Y\tilde{U}_Y \right) - v_X \tilde{U}_X - v_Y \tilde{U}_Y + \left(\tilde{U}_{XX} + \tilde{U}_{YY} + \tilde{U}^p \right)_X = 0, \tag{18}$$

where the sub/superscript ∞ denotes that the quantity is taken in the limit as $T \rightarrow \infty$ and \tilde{U} stands for a blow-up profile.

Two possible stable blow-up mechanisms are expected in KdV-type equations: either an algebraic dependence of L on T , or an exponential one. In the former case, the quantity \tilde{a} in (17) will vanish, and Eq. (18) will be identical to the equation for the soliton if $v_Y = 0$; this mechanism is expected in the L^2 -critical case. If $L \propto 1/T$

as in the L^2 -critical gKdV case, recalling (15), we get

$$L \propto \sqrt{t^* - t}. \quad (19)$$

In the supercritical case, one expects an exponential decay of L with T , that is, $L \propto \exp(-\gamma T)$ with $\gamma > 0$, and from (15) we have

$$L \propto (t^* - t)^{1/3}. \quad (20)$$

In our simulations, we trace the L^∞ norm of u , the L^2 norm of u_x and in the L^2 -critical case the velocity v_x . The first two norms are proportional to $L^{\frac{2}{p-1}}(t)$ via rescaling in (15), see details in Sects. 4 and 5. We also note that this is similar to the blow-up situation in NLS-type equations, for example, see Yang et al. (2019) and Sulem and Sulem (1999).

3 The L^2 -Subcritical Case

In this section, we study the ZK equation in the subcritical case $p = 2$. We consider the stability of the solitons, the interaction of solitons and the appearance of solitons in the long-time evolution of general localized initial data.

We work with $L_x = L_y = 10$ and $N_x = N_y = 2^{10}$ Fourier modes and $N_t = 2000$ time steps on the considered time intervals. In all studied cases, the Fourier coefficients decrease at least to the order of 10^{-5} , and the relative energy is conserved at least to the same order (except for the examples in the last subsection, these numbers are in general of the order of 10^{-10}). This means that the numerical error is in all cases much smaller than plotting accuracy.

The results of this section give positive confirmation to the Conjecture 1.

3.1 Soliton Stability

We first address stability of solitons by considering initial data of the form $u_0 \equiv u(x, y, 0) = \lambda Q(x, y)$, $\lambda \in \mathbb{R}$. We use a co-moving frame, i.e., we solve

$$u_t + (u_{xx} + u_{yy} + u^p - vu)_x = 0, \quad p = 2, 3, 4, \quad (21)$$

with $v = 1$.

The solution to (1) with $\lambda = 1.1$ can be seen at $t = 15$ on the left of Fig. 3. The perturbed soliton (with $u_0 = 1.1Q$) visibly moves faster than the original soliton ($u_0 = Q$), since it is not stationary in the co-moving frame. There is also some radiation propagating into the negative x -direction (which is more visible in Fig. 5). The L^∞ norm of the solution on the right of Fig. 3 also appears to saturate at a higher value than the initial value. Thus, it seems that the perturbation with higher mass than the original soliton leads to a larger and faster moving to the right soliton and some radiation moving to the left.

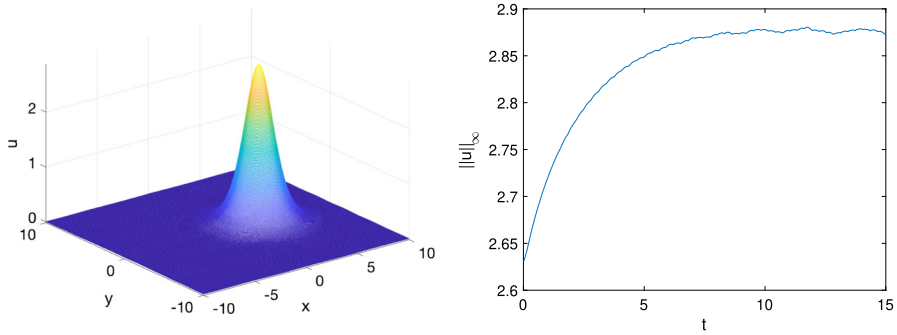


Fig. 3 Solution to (1) with $u(x, y, 0) = 1.1Q(x, y)$: on the left the solution at $t = 15$; on the right the L^∞ norm of the solution depending on time

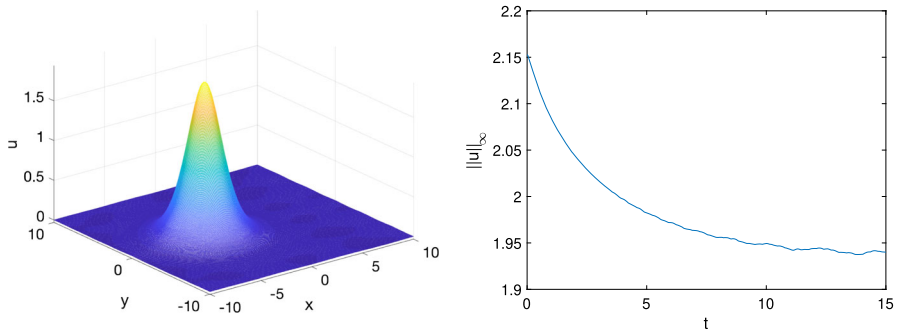
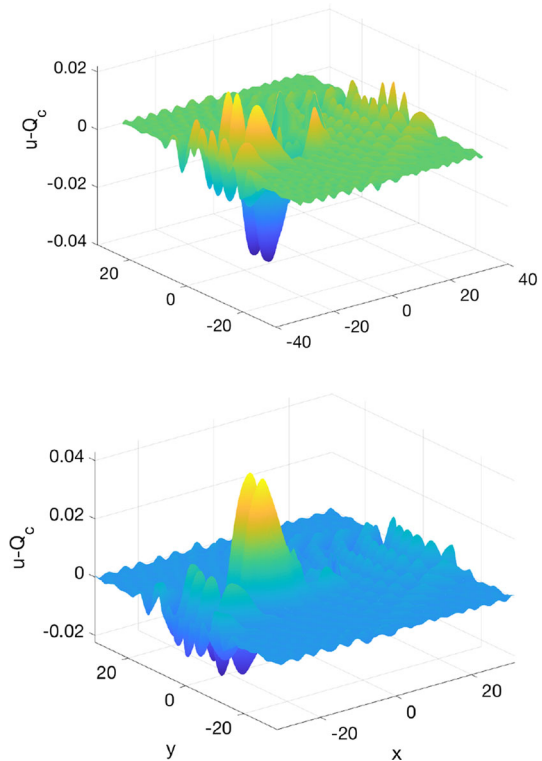


Fig. 4 Solution to (1) with $u(x, y, 0) = 0.9Q(x, y)$: on the left the solution for $t = 15$; on the right the L^∞ norm of the solution depending on time

On the other hand, a perturbation with smaller mass ($u_0 = 0.9Q$) is shown on the left of Fig. 4. The fact that the hump moves to the left of the origin in the co-moving frame indicates that the resulting soliton has even smaller mass than the perturbed one. This is in accordance with the L^∞ norm of this solution shown on the right of Fig. 4: it appears to decrease to a lower height than the initial value. Thus, the perturbed initial data of a mass smaller than the perturbed soliton seem to lead to a soliton of smaller mass plus radiation. Figures 3 and 4 indicate that the ZK soliton is stable, as expected, when $p = 2$.

Remark 3.1 Note that in this paper we systematically approximate situations on \mathbb{R}^2 by a setting on \mathbb{T}^2 . Within machine precision, this does not make a difference for stationary localized solutions as the solitons of the ZK equation, if the periods are chosen sufficiently large. However, if radiation appears, as it happens in this and in the following sections, one would have to choose prohibitively large computational domains to avoid the reappearance of emitted radiation (always emitted in the negative x -direction) for positive values of x . This is acceptable as long as this radiation has much smaller amplitudes than the studied bulk of the solution. Effects of the radiation are shown in Figs. 3 and 4 in the variations of the L^∞ norms for large times (this is also connected with the determination of the L^∞ norm on a discrete grid, which

Fig. 5 Difference of the solution to (1) with $u(x, y, 0) = \lambda Q(x, y)$ and a fitted rescaled soliton from (6): on the left $\lambda = 0.9$; on the right $\lambda = 1.1$



means that the real location of the maximum of the solution might not be on a grid point).

One may ask to which extent the final states of the solutions shown in Figs. 3 and 4 are solitons if the radiation cannot escape the computational domain. To address this question, we show in Fig. 5 the difference between the solutions for $t = 15$ and a fitted soliton rescaled according to (6) (c is determined via $c = \|u\|_\infty / \|Q\|_\infty$). In Fig. 5, one can clearly see how the radiation forms a background in the computational domain, and that the difference between the bump and a soliton is smaller than the radiation background. Thus, the conclusion that the final state is a soliton plus radiation escaping on \mathbb{R}^2 to infinity is justified. Even more can be seen in the previous figures: the radiation escapes to the ‘left’ of the moving rightward solution at an angle of 30° with the negative x -axis (for a total opening of 60°). This is in confirmation of the asymptotic stability result in Côte et al. (2016).

3.2 Soliton Interaction

Since the soliton solutions are rapidly decreasing for $x^2 + y^2 \rightarrow \infty$, one can study their interactions by considering initial data which are the sum of displaced solitons. This allows the study of multi-soliton solutions to what is clearly a non-integrable equation.

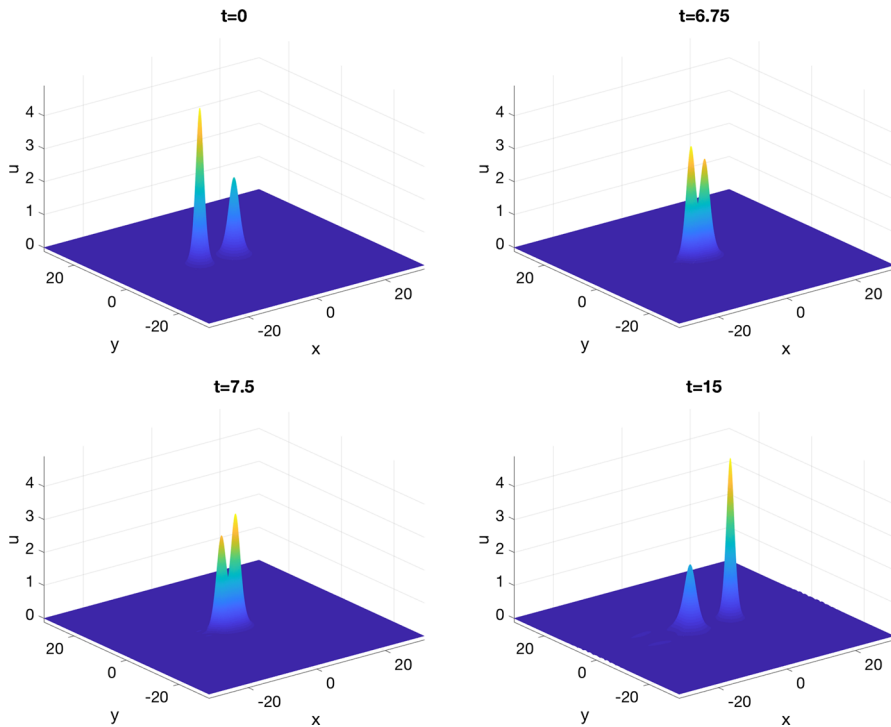


Fig. 6 Snapshots of the solution to (1) with the initial condition being a superposition of the soliton with $c = 2$ centered at $x = -10$ and a soliton with $c = 1$ centered at the origin

Initial data can be constructed by superimposing two one-soliton solutions that are sufficiently far. Indeed, since solitons have an exponential decay, their contribution far away from their joint center of mass is zero within the numerical precision.

As shown in Fig. 6 on the left of the first row, we consider the initial condition with two localized but somewhat separated solitons: one of them is the soliton (6) with $c = 2$ centered at $x = -10$ and another one is with $c = 1$ centered at the origin. In our simulations, we actually solve (5) with $c = 2$ to obtain the appropriate soliton; however, as an alternative, we could have used the scaling property (6) to get the soliton with $c = 2$.

Figure 6 shows that the faster soliton (note that we are still in a co-moving frame with $c = 1$) will hit the slower soliton around $t = 7$. The collision is essentially elastic; the solitons appear to keep their shape after the collision.

The collision is best seen in a video (see Video Gallery), or on the x -axis as shown in Fig. 7, since the motion is exclusively in the x -direction. In Fig. 7, we show the profile of this 2-soliton solution on the x -axis for various times. We note that the figure (except for the small radiation toward infinity) resembles closely the KdV 2-soliton. However, the appearance of some radiation as seen from the close-up (right subplot) of the bottom right figure of Fig. 6 shows that the ZK equation is indeed not integrable.

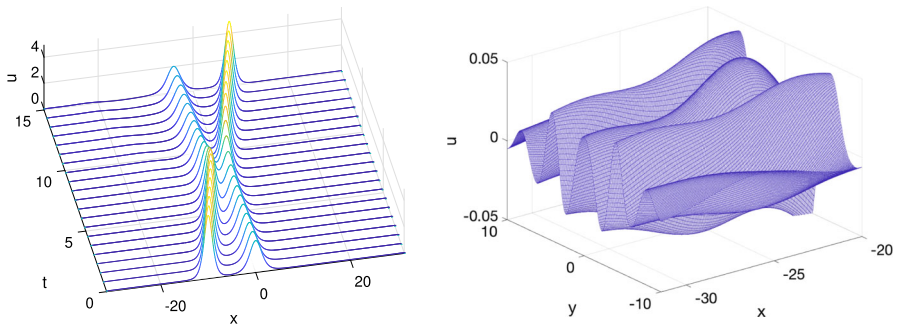


Fig. 7 Solution to (1) with $u(x, y, 0)$ being the superposition of a soliton with $c = 2$ centered at $x = -10$ and a soliton with $c = 1$ centered at the origin on the x -axis for various times on the left, and a close-up of the bottom right subplot of Fig. 6 (at $t = 15$) on the right

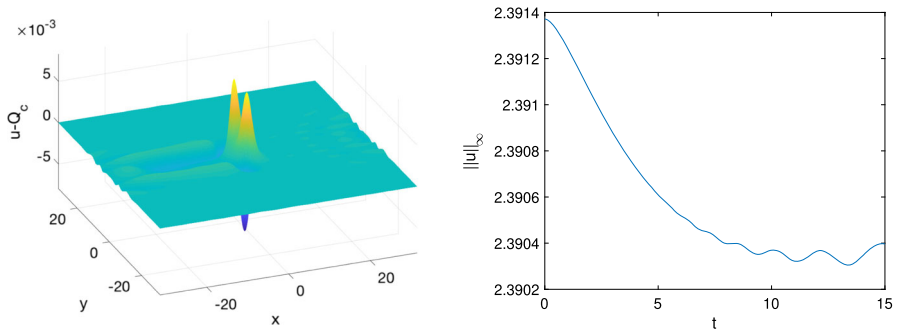


Fig. 8 Solution to (1) with $u(x, y, 0) = Q(x, y - a) + Q(x, y + a)$ and $a = 5$; on left the difference of the numerical solution at $t = 15$ and the initial data, on the right the L^∞ norm of the solution

Next, we consider initial data of the form $u(x, y, 0) = Q(x, y - a) + Q(x, y + a)$ with $a > 0$ a constant in order to study how the solitons interact if they have equal speeds, but are separated in the y -direction. In Fig. 8, we show the difference of the solution for $a = 5$ at $t = 15$ and the initial data in a co-moving frame with $c = 1$. In this case, the value of each soliton at the maximum of the other is on the order of 10^{-4} . The interaction is therefore minimal, and the difference shown in Fig. 8 on the left is of the order of 10^{-3} .

The snapshots of the solution for the same initial data with $a = 2$ are shown in Fig. 9 at different times.

It appears that the final state of the solution is a single soliton. This is indicated both by the L^∞ norm of the solution on the left subplot of Fig. 10 and by the difference with a fitted soliton solution of (6) on the right subplot.

We next note that if we consider a slightly off-centered collision of solitons, that is, the solution with the initial condition $u(x, y, 0) = Q_2(x + 10, y + 1) + Q(x, y)$, we get a very similar behavior to the collision in Fig. 7, see snapshots in Fig. 11. After the interaction, the larger soliton, which was below the smaller one in the y -direction, will be above it (they essentially change roles in the elastic collision).

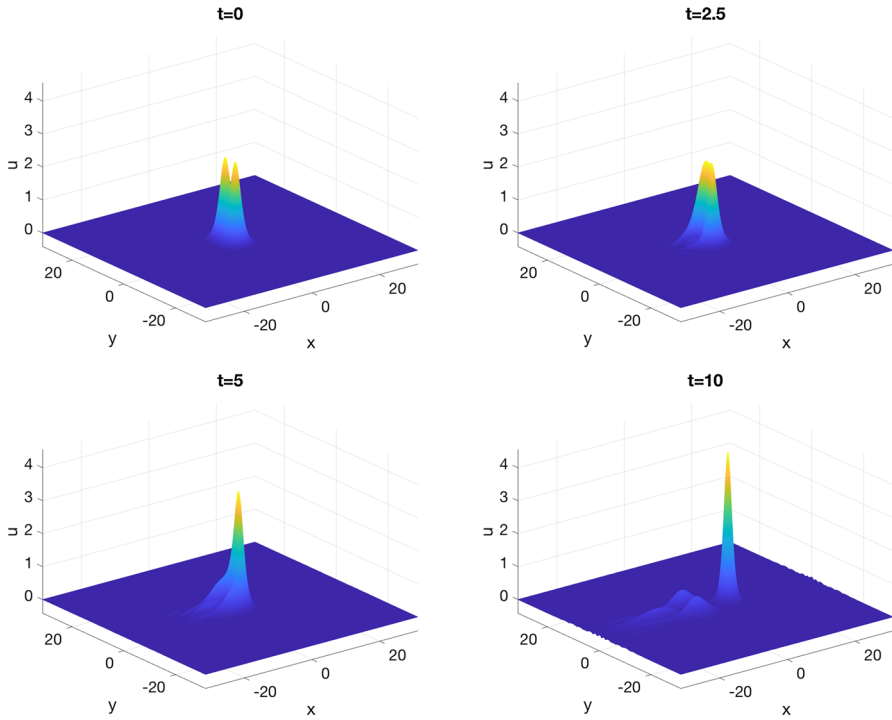


Fig. 9 Snapshots of the solution to (1) with $u(x, y, 0) = Q(x, y - a) + Q(x, y + a)$ and $a = 2$ at different times

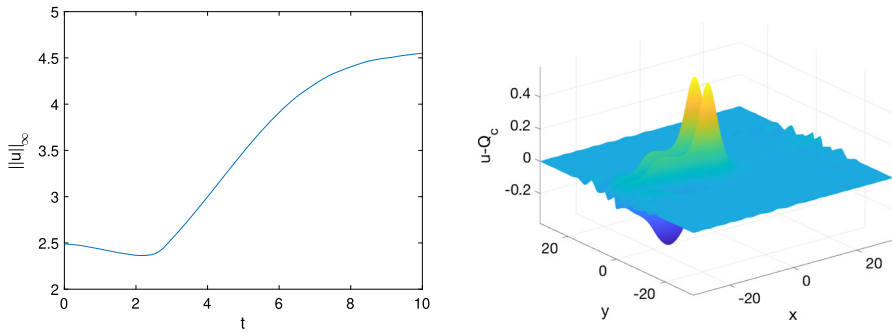


Fig. 10 L^∞ norm of the solution to (1) with $u(x, y, 0) = Q(x, y - a) + Q(x, y + a)$ and $a = 2$ on the left; the difference between this solution at $t = 10$ and a fitted soliton solution of (6) on the right

We thus conclude that it is the separation distance, not the relative location in the plane, of solitons that influences their interaction in the long run. This dependence is of significant interest, but will be investigated elsewhere.

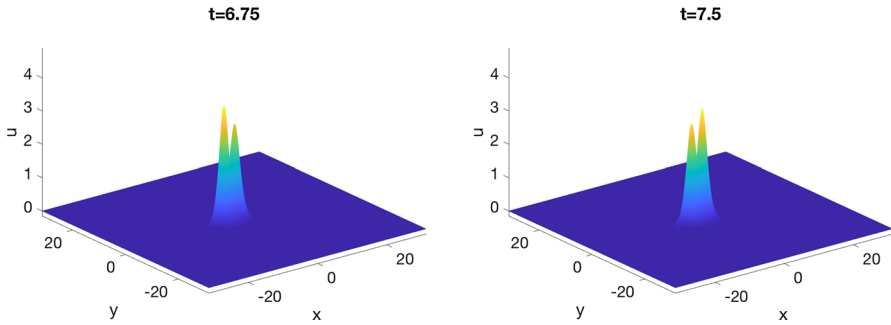


Fig. 11 Solution to (1) with $u(x, y, 0) = Q_2(x + 10, y + 1) + Q(x, y)$ slightly before and after the collision of the solitons

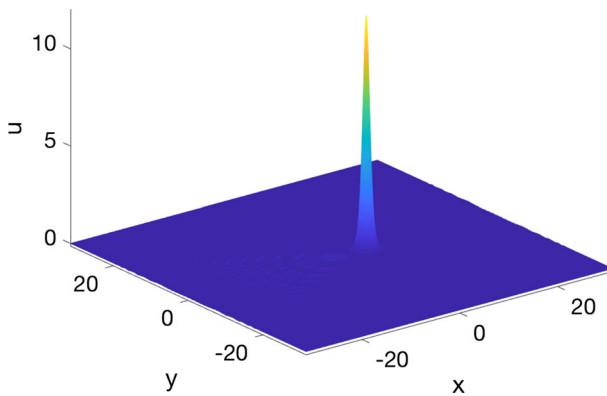


Fig. 12 Solution to (1) with $u(x, y, 0) = 10 e^{-(x^2+y^2)}$ at $t = 1$. Note the radiation emitted to the left with the total angle of 60°

3.3 Soliton Resolution

Since ZK solitons in the subcritical case $p = 2$ are clearly stable (from what we simulated both orbitally and asymptotically), and furthermore, they even show essentially elastic collisions, one would expect that, according to the soliton resolution conjecture, solitons plus radiation appear in the long term evolution of localized initial data with sufficient mass. For the following computations in this subsection, we no longer use co-moving frames.

In Fig. 12, we show the ZK evolution (at $t = 1$) of the Gaussian initial condition $u(x, y, 0) = 10 e^{-(x^2+y^2)}$. It appears that a single soliton emerges from the initial bump plus some radiation. We note that the radiation is emitted to the left of the x -axis up to an angle of 30° with the negative x -axis (so the total opening is 60°); this is in confirmation of the results in Côté et al. (2016).

The L^∞ norm of the solution shown on the left in Fig. 13 also indicates that a soliton appears. The difference between the numerical solution at $t = 1$ and a fitted soliton solution of (6) can be seen on the right of the same figure. It indicates that a

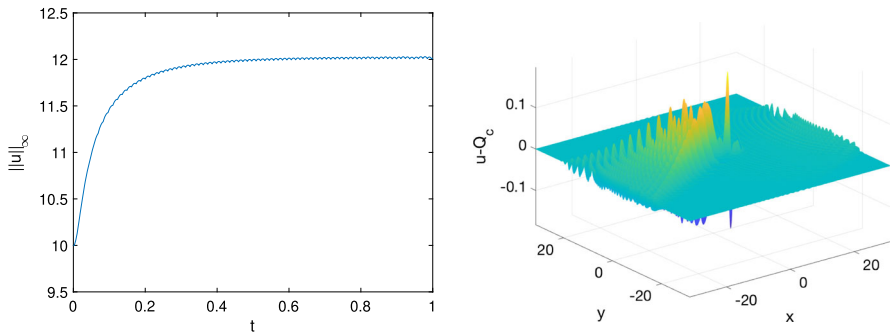


Fig. 13 Solution to (1) with $u(x, y, 0) = 10e^{-(x^2+y^2)}$: on the left the time dependence of the L^∞ norm of the solution; on the right the difference between the solution at $t = 1$ and a fitted soliton

soliton appears, but that the final state has not yet been reached, which is also clear from the presence of radiation in the figure.

Since we have shown in Fig. 9 that nearby solitons tend to merge into a single soliton, it is not surprising that the same is found for nearby general bumps. Therefore, it is interesting to study initial data with an extended maximal region, for instance, the wall-like structure

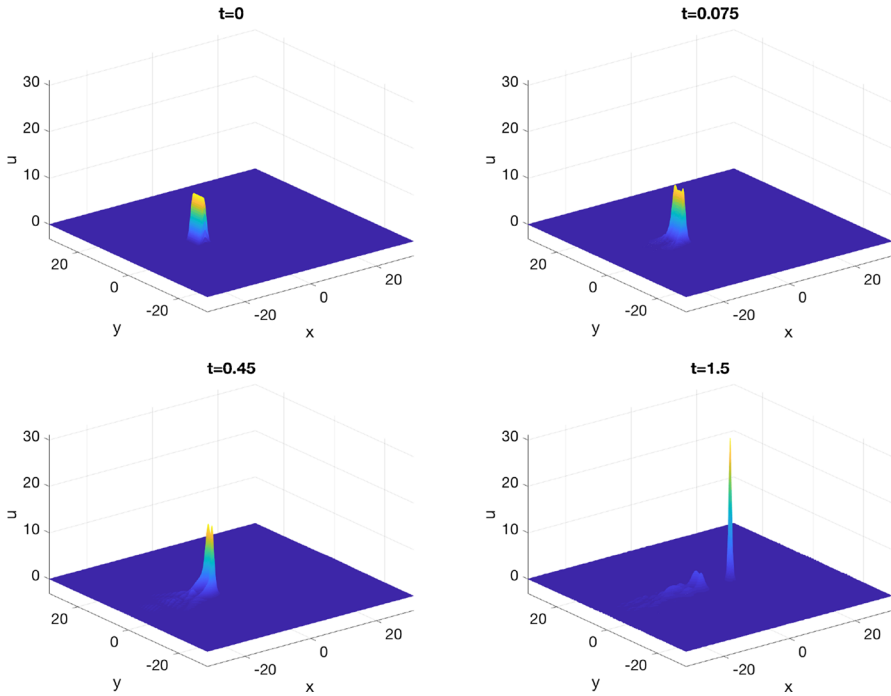


Fig. 14 Time snapshots of the solution to (1) with the wall-type initial condition (22)

$$u(x, y, 0) = \begin{cases} 10 e^{-x^2} & |x| \leq 1.5 \\ 10 e^{-(x^2+(y-1.5)^8)} & x > 1.5 \\ 10 e^{-(x^2+(y+1.5)^8)} & x < -1.5. \end{cases} \quad (22)$$

The snapshots at different times of the corresponding ZK solution are given in Fig. 14. The initial wall develops two peaked structures near the edges, which then merge into one large bump traveling to the right, and radiation (and possibly forming more smaller solitons, traveling slowly behind).

The L^∞ norm on the left of Fig. 15 appears to be still slightly growing, which indicates that the final state of the main bump is not yet reached. Note, however, the difference to a fitted soliton solution of (6) makes a plausible conclusion that this final state should indeed be a soliton.

From the previous simulations, it is not yet clear whether more than one soliton can appear in the long term evolution of such data. To address this question, we consider once more initial data with a broad maximum; for example, we take $u(x, y, 0) = 25 e^{-(x^2+0.05y^2)}$. The solution at $t = 0.5$ is plotted on the left of Fig. 16. It looks as if several solitons appear in this case. On the right subplot, we demonstrate the difference with a soliton fitted to the first bump, which appears to be close to a soliton. One would have to run simulations for much longer times in order to decide how many solitons will appear in the asymptotic solution.

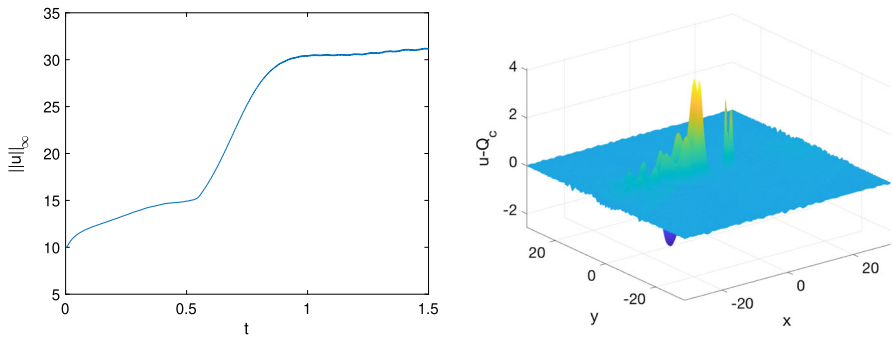


Fig. 15 Solution to (1) with u_0 in (22): on the left time dependence of the L^∞ norm; on the right the difference between the solution at $t = 1.5$ and a fitted soliton

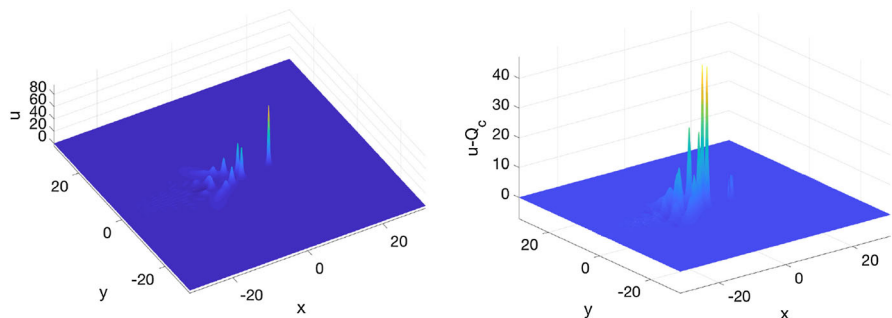


Fig. 16 Solution to (1) with $u(x, y, 0) = 25 e^{-(x^2-0.05y^2)}$ at $t = 0.5$ on the left, and on the right the difference between this solution and a fitted (to the first bump) soliton

Therefore, the soliton resolution conjecture seems to hold for the 2D subcritical ZK equation: in the long-time behavior of solutions with sufficiently regular and sufficiently localized initial data only solitons and radiation appear.

4 The L^2 -Critical Case

Since it is known that the direct integration of (16) with Fourier methods is challenging, we instead integrate (1) and trace certain norms of the solution. It is expected, see Farah et al. (2018), that a blow-up is observed as $x \rightarrow \infty$. Therefore, we keep the term x_m in (16) and solve (13) as follows: we choose x_m in such a way that the maximum of the solution is at $x = x_0, y = 0$ for all times. The quantity x_0 is chosen so that the radiation, propagating in negative x -direction, will hit the computational boundary (because of the imposed periodicity) only at a time shortly before the blow-up time, thus, its influence on the blow-up is negligible.

We study perturbations of the soliton as in the previous section and Gaussian initial data. The results of this section confirm Conjecture 2, which in some sense resembles the 1D critical gKdV equation. In particular, the gKdV examples showed that the

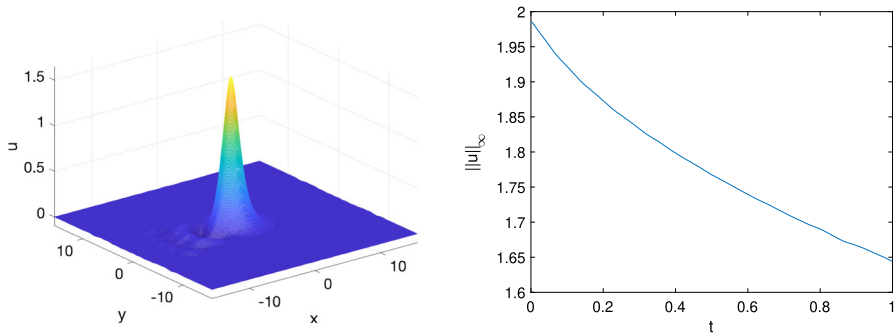


Fig. 17 Solution to (1) with $u(x, y, 0) = 0.9Q(x, y)$ at $t = 1$ on the left and its L^∞ norm depending on time on the right

blow-up mechanism for the studied norms (L^2 or L^∞) can be well captured; the more challenging task is to understand the velocity of the blow-up profile.

4.1 Perturbations of the Soliton

We start investigating the evolution of the ZK flow with initial data of perturbed solitons, of the form $u(x, y, 0) = \lambda Q(x, y)$, where Q is the numerically constructed soliton solution to (5) with $c = 1$. We start with $u(x, y, 0) = 0.9 Q(x, y)$. A snapshot plotted at $t = 1$ of the ZK evolution with this initial data is plotted on the left subplot of Fig. 17. The right subplot shows the L^∞ norm depending on time, which appears to be monotonically decreasing; therefore, this solution disperses to infinity (of course, one could debate if the L^∞ norm ever stabilizes at a certain value, as for example in Fig. 4, in the present situation we see that the L^∞ norm has a definite negative slope and that there is no increase after some time as in the stable cases). One could run this example for longer times, but since we approximate situations in \mathbb{R}^2 by simulations on torus, the L^∞ norm can never tend to zero, but will saturate at the level of the noise; this question should also be investigated analytically. In our simulations, because of the imposed periodicity, radiation (propagating toward negative values of x) reenters the computational domain on the right after some time (and hence, we have to stop our simulations at a certain time). We also note that dispersion propagates leftward in some wedge around the negative x -axis (30° as shown in Côte et al. (2016)). Therefore, we conclude that the soliton is unstable against dispersion, as expected, for perturbations with a smaller mass than that of the soliton.

Perturbations of solitons with larger mass, for instance, with the initial condition $u(x, y, 0) = 1.1 Q(x, y)$, lead to a blow-up solution with various diverging norms. To approach this blow-up whilst maintaining at least plotting accuracy, we run the code first with $N_x = N_y = 2^{10}$ Fourier modes and $N_t = 2000$ time steps for $t < 2.6$. The snapshot of this ZK evolution at $t = 3$ is shown in Fig. 18 on the left. Noting that the height of the bump is already at least 3 times larger than the initial height, implies that the soliton is unstable: a strong peak has formed (and moving with an increasing speed) as well as some bulk of radiation propagating in the negative wedge

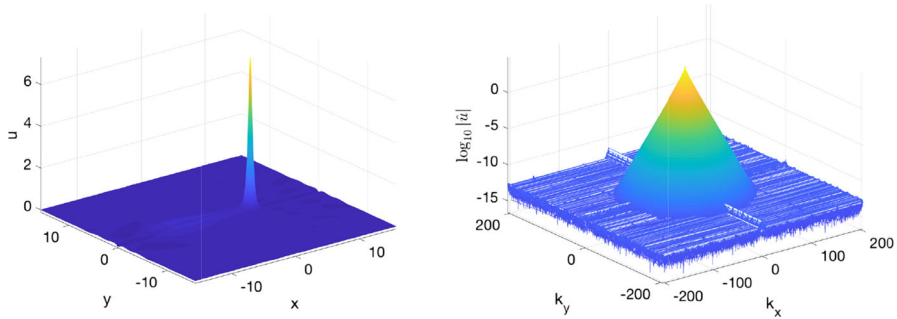


Fig. 18 Solution to (1) with $u(x, y, 0) = 1.1Q(x, y)$ at $t = 2.6$ on the left, and the Fourier coefficients on the right

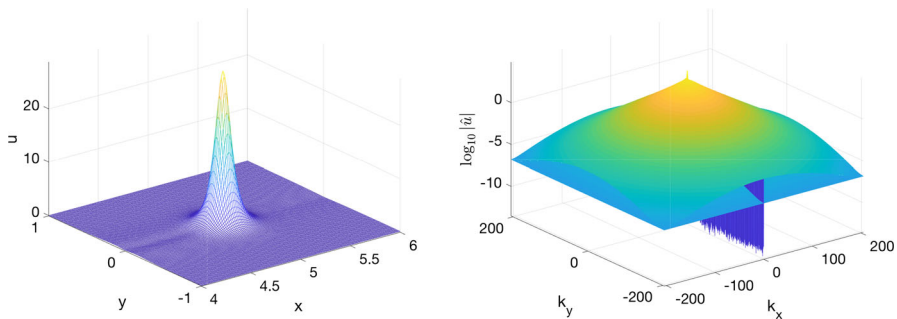


Fig. 19 Solution to (1) with $u(x, y, 0) = 1.1Q(x, y)$ at $t = 3.1445$ on the left, and the corresponding Fourier coefficients on the right

of the x -direction (recall that we are in a frame co-moving with the maximum, which is kept fixed at $(x_0, 0)$). The Fourier coefficients of the solution on the right of Fig. 18 indicate that it is resolved to the order of the rounding error.

The solution shown in Fig. 18 is then used as the initial condition for an ensuing computation with $N_x = N_y = 2^{11}$ and $N_t = 10^4$ time steps for $t \leq 0.55$. The code breaks at $t \sim 0.541$. In Fig. 19, we show the solution at the last recorded time $t = 0.5445$ on the left. The Fourier coefficients on the right of the same figure indicate that there is still spatial resolution beyond plotting accuracy at that time. This means that (similar to the case of blow-up in the Novikov–Veselov equation, see Kazeykina and Klein (2017)) the resolution is first lost in time (compare this to the case of blow-up solutions for the DS II system (Klein and Stoilov 2018), where the limiting factor is spatial resolution). The loss of resolution in time leads eventually to a breaking of the code.

The divergence of the L^∞ norm of the solution $u(t)$ and of the L^2 norm of $u_x(t)$ (shown in Fig. 20) confirms the blow-up behavior. Furthermore, the growth of the norms in Fig. 20 provides information on the blow-up mechanism. Assuming that the blow-up core (the first bump) has a self-similar structure (a dynamic rescaling of the Q profile), we fit various norms $g(t)$ close to the blow-up time to the following law

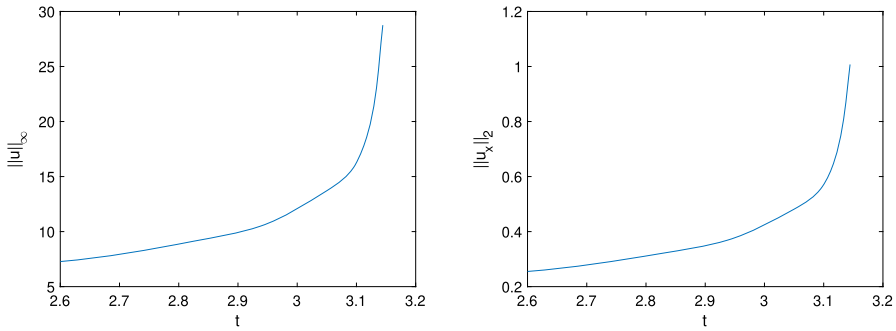


Fig. 20 Solution to (1) with $u(x, y, 0) = 1.1Q(x, y)$: on the left the L^∞ norm of the solution; on the right the L^2 norm of u_x

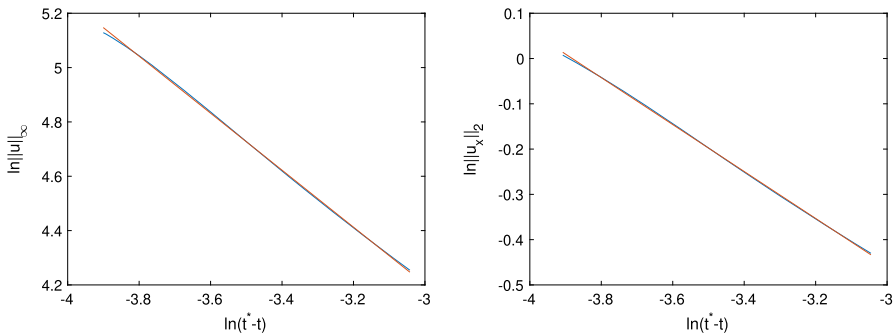


Fig. 21 Fitting of various norms of the solution to (1) with $u(x, y, 0) = 1.1Q(x, y)$ to $\ln g(t) \sim a \ln(t^* - t) + b$: on the left the L^∞ norm of the solution fitted to $y = -0.4824x + 1.4266$; on the right the L^2 norm of u_x fitted to $y = -0.5185x - 2.0124$; in red the fitted line

$$\ln g(t) \sim a \ln(t^* - t) + b. \tag{23}$$

This fitting is done for the last 500 recorded time steps implementing the algorithm Lagarias et al. (1998) in MATLAB as *fminsearch*. Here the obtained results do not change significantly if slightly more or less points are used for the fitting. For the L^∞ norm we find $a = -0.4824$, $b = 1.4266$ and $t^* = 0.5625$. For the L^2 norm of u_x , we get $a = -0.5185$, $b = -2.0124$ and $t^* = 0.5646$. The quality of both fittings is shown in Fig. 21.

The growth of the quantity v_x as in (13), the speed of the frame co-moving with the maximum (see (18)), is shown on the left of Fig. 20, which suggests that the blow-up takes place at infinity. Fitting to $\ln v(t) \sim a \ln(t^* - t) + b$, we find $a = -1.0491$, $b = 1.0553$ and $t^* = 0.5647$. Note the agreement of the blow-up times, which shows the consistency of the used approach, though as mentioned in Remark 1.1, it is rather difficult to identify the blow-up rate of the velocity (Fig. 22).

To numerically determine the blow-up profile, we compute the quantity \tilde{u} , representing the limiting object in Conjecture 2. To do this, we numerically determine the maximum and its location and determine via interpolation the dynamically rescaled soliton Q according to (7). The result is shown in Fig. 23. Remarkably, the difference

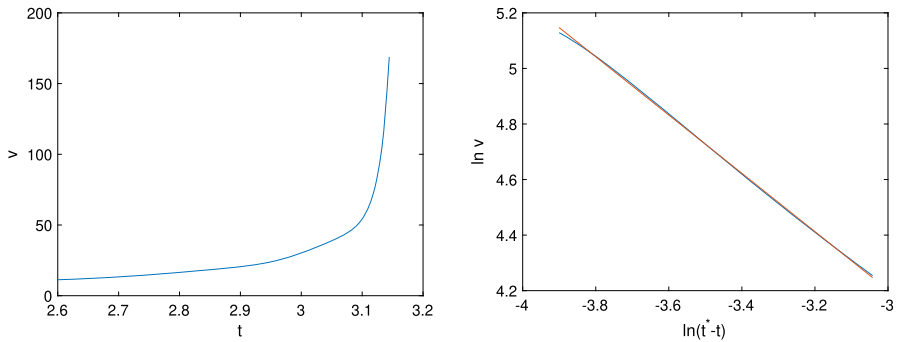


Fig. 22 Solution to (1) with $u(x, y, 0) = 1.1Q(x, y)$; on the left time dependence of v_x ; on the right a fitting to $\ln v(t) \sim a \ln(t^* - t) + b$

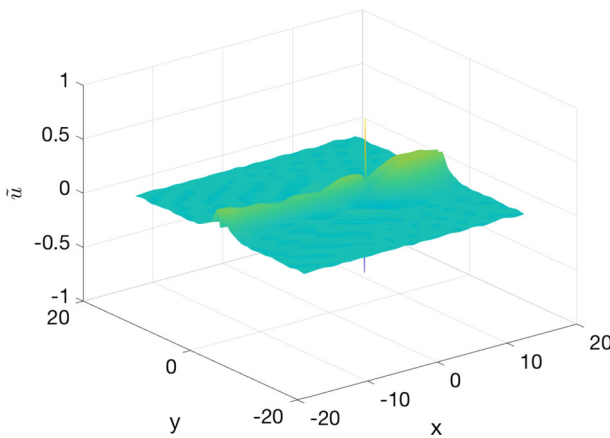


Fig. 23 The quantity \tilde{u} in Conj. 2 giving the blow-up profile for the solution to (1) with $u(x, y, 0) = 1.1Q(x, y)$ at $t = 3.1445$

between the expected and computed blow-up profile is of the same order as the radiation profile. This indicates that the numerical estimate accurately represents the actual blow-up.

4.2 Gaussian Initial Data

Formation of blow-up in finite time can be observed not only for perturbations of the soliton, but for more general initial data. We illustrate this on an example with Gaussian initial data, $u(x, y, 0) = \lambda e^{-(x^2+y^2)}$. For smaller λ , for instance $\lambda = 2$, the evolution is dispersed. For $\lambda = 3$, the evolution blows up in finite time. To study this, we use again $N_x = N_y = 2^{10}$ Fourier modes on $5[-\pi, \pi] \times 5[-\pi, \pi]$ and $N_t = 2000$ time steps for $t \leq 0.5$. The resulting solution is then taken as the initial condition for an ensuing computation with $N_x = N_y = 2^{11}$ Fourier modes and $N_t = 10^4$ time steps for $t \leq 0.42$. The code breaks at $t = 0.4175$. The solution at this specific time

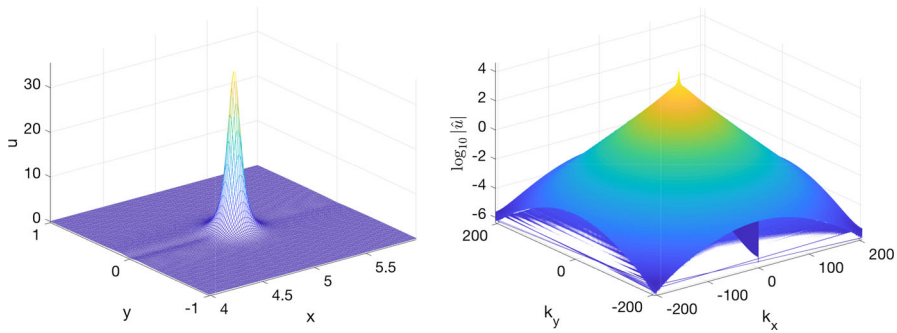


Fig. 24 Solution to (1) with $u(x, y, 0) = 3 e^{-(x^2+y^2)}$ at $t = 0.9175$ on the left, and the corresponding Fourier coefficients on the right

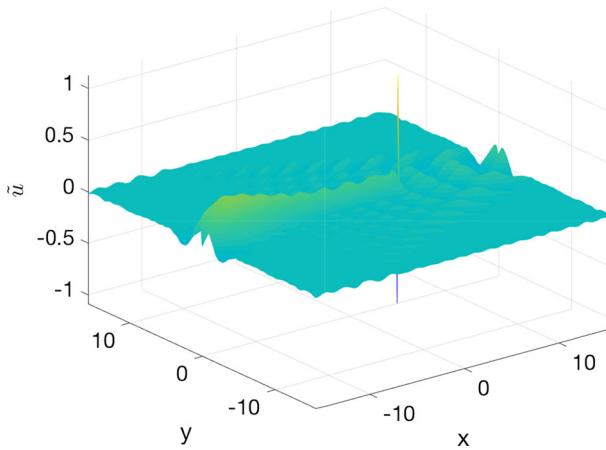


Fig. 25 Quantity \tilde{u} in Conj. 2 giving the blow-up profile for the initial condition $u(x, y, 0) = 3 e^{-(x^2+y^2)}$ at $t = 0.9175$

is shown in Fig. 24 on the left. The Fourier coefficients for this time are given on the right of the same figure and show that the solution is still well resolved in the Fourier domain. Thus again, one runs out of resolution in time with the KdV-type equations.

The L^∞ norm of u , the L^2 norm of u_x and the velocity v_x appear to blow-up. Fitting these norms as before to the law (23) for the last 500 recorded time steps gives $a = -0.53, b = 1.44$ and $t^* = 0.9436$ for the L^∞ norm of u , $a = -0.64, b = -0.73$ and $t^* = 0.944$ for the L^2 norm of u_x , and $a = -1.4, b = 0.49$ and $t^* = 0.9446$ for the v_x . The fitting errors are slightly larger than in the case of the perturbed soliton studied above (on the order of a few percent for the norms, though around 20% for the velocity, which as we mentioned before is difficult to trace). However, there is a good agreement of the fitted blow-up times in all cases.

The blow-up profile appears to be again a dynamically rescaled soliton Q as in Conjecture 2, see Fig. 25 for the residual. The residual (in the center) slightly above the radiation background shows that the final phase of the blow-up is close, though not yet fully reached.

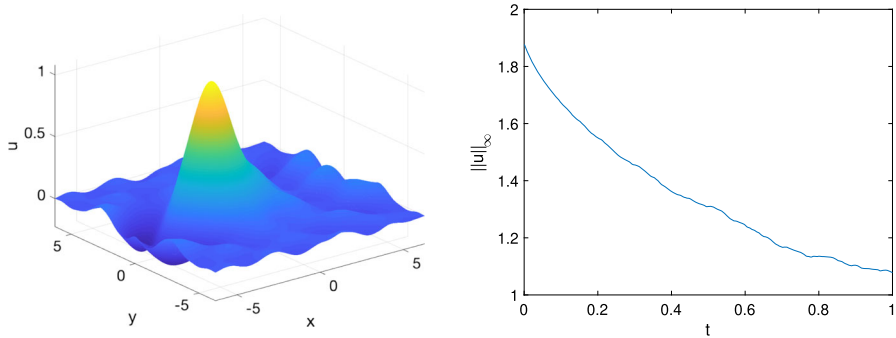


Fig. 26 Solution to (1), $p = 4$, with $u(x, y, 0) = 0.9Q(x, y)$ at $t = 1$ on the left, and time dependence of the corresponding L^∞ norm on the right

5 The L^2 -Supercritical Case

In this section, we study the L^2 -supercritical case. As far as the rates of blow-up are concerned, it is numerically less challenging than in the critical case, since the blow-up happens on smaller time scales and centered at finite values of x . Though blow-up is always numerically challenging, at least some of the complications from the L^2 -critical case are absent. As in the previous section we study perturbations of the soliton and Gaussian initial data. In this section we give positive confirmation to Conjecture 3.

5.1 Perturbations of the Soliton

As in the previous sections, we first study the stability of the soliton by considering initial data of the form $u(x, y, 0) = \lambda Q(x, y)$, $\lambda > 0$ in a co-moving frame with $c = 1$.

We start with the case $\lambda = 0.9$ for $t = 0$. The solution at $t = 1$ is shown in Fig. 26 on the left. The soliton is clearly unstable and disperses as time increases. Since we work on \mathbb{T}^2 here, the radiation cannot escape to infinity and forms a noisy background, into which the soliton will finally disappear. The time dependence of the L^∞ norm of the solution is plotted on the right of Fig. 26. The norm is monotonically decreasing (the ripples being due to radiation reappearing on the other side of the computational domain and interacting then with the remaining peak).

When $\lambda = 1.1$, we use a smaller computational domain than in the L^2 -critical case, since the blow-up will happen at finite values of x and y . In practical terms this means that the blow-up profile will stay close to the bulk of the radiation. Thus, we can work on the domain $2[-\pi, \pi] \times 2[-\pi, \pi]$. Consequently we operate with much higher spatial resolution than in the previous section, where we used a considerably larger domain. We use $N_x = N_y = 2^{10}$ Fourier modes and $N_t = 20000$ time steps for $t \leq 0.17$. The code breaks at $t = 0.1674$. The solution at the final recorded time can be seen on the left of Fig. 27. The Fourier coefficients of the solution at the final time are shown on the right of the same figure. Note that the solution is still very well

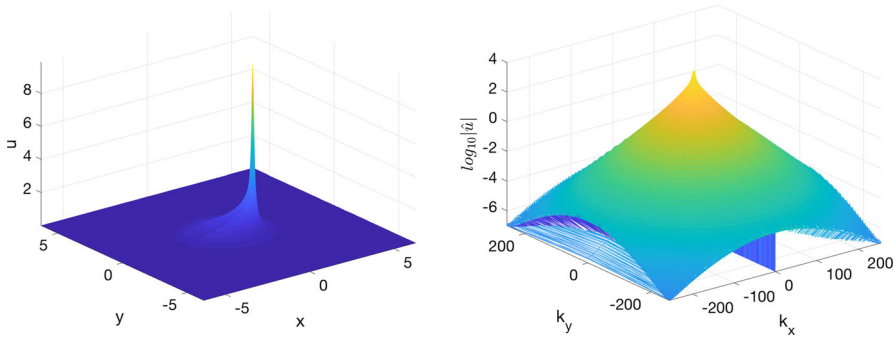


Fig. 27 Solution to (1), $p = 4$, with $u(x, y, 0) = 1.1Q(x, y)$ at $t = 0.1674$ on the left, and the corresponding Fourier coefficients on the right

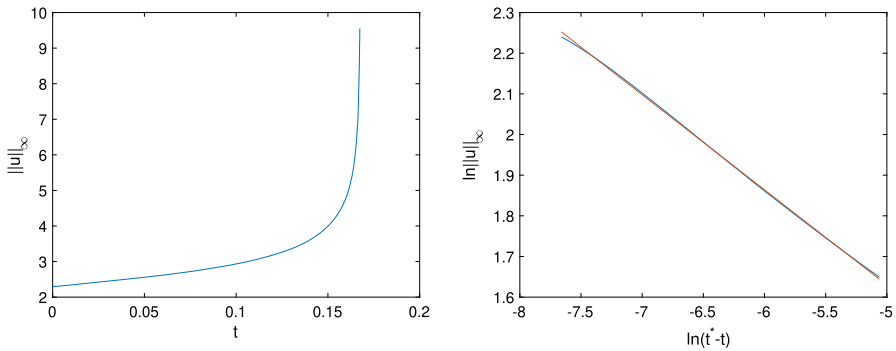


Fig. 28 L^∞ norm of the solution to (1), $p = 4$, with $u(x, y, 0) = 1.1Q(x, y)$ on the left, and a fit to $\ln g(t) \sim a \ln(t^* - t) + b$ on the right (in red the fitted line)

resolved spatially, though the code breaks a few time steps after the last recorded one. Thus, again the resolution in time is the limiting factor in blow-up computations for ZK.

The L^∞ norm of the solution is shown in Fig. 28. It can be seen that the blow-up happens on much smaller time scales than in the critical case. A fit of the norm for the last 500 recorded time steps to $\ln g(t) \sim a \ln(t^* - t) + b$ yields $a = -0.22$ $b = 0.48$ and $t^* = 0.1678$. We observe that the result is virtually the same if we only fit the last 100 time steps. This is in accordance with the expectation that the power exponent for the blow-up rate $u_x(t)$ in terms of $t^* - t$ is $a = \frac{2}{9} = \frac{1}{3} \cdot \frac{2}{3} \approx 0.22$, see Conjecture 3, (10).

The figures for the growth of the L^2 norm of u_x are very similar to the ones for the L^∞ norm of u ; therefore, we do not present them here. The fitting of this norm for the last 500 time steps gives $a = -0.22$, $b = -0.38$ and $t^* = 0.1678$ with a fitting error of the order of 10^{-4} . The excellent agreement of the results by both norms confirms that the results for the blow-up in the L^2 -supercritical case are more accurate and more stable than in the critical case.

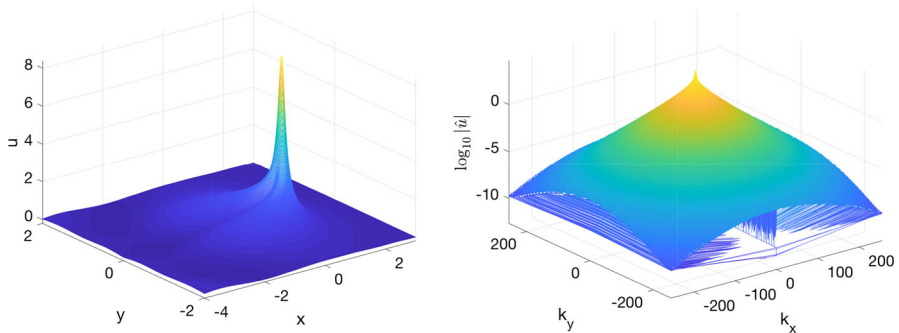


Fig. 29 Solution to (1), $p = 4$, with $u(x, y, 0) = 1.1Q(x, y)$ at $t = 0.1399$ on the left, and the corresponding Fourier coefficients on the right

5.2 Gaussian Initial Data

Finally, we consider Gaussian initial data of the form $u(x, y, 0) = \lambda e^{-(x^2+y^2)}$ with $\lambda > 0$ in a stationary frame. First we observe that for smaller λ (for instance $\lambda = 1$) the initial bump is dispersed similar to the L^2 -critical case of the perturbed soliton with the initial mass smaller than the soliton mass.

For larger λ , the evolution blows up in finite time. For example, for $\lambda = 2$, we use the same parameters as for the blow-up computation in the previous subsection. The code breaks at $t = 0.1399$. The ZK solution at that time is shown in Fig. 29.

Fitting of the norms is of the same quality as shown in Fig. 28. We find the fitting to the law (23) for the L^∞ norm of u gives the values $a = -0.229$, $b = 0.45$ and $t^* = 0.1405$ with a fitting error of the order of 10^{-2} . For the L^2 norm of u_x , we get $a = -0.216$, $b = -0.39$ and $t^* = 0.1405$ with a fitting error of the order of 10^{-4} .

The results of this and previous subsections give strong evidence in support of Conjecture 3: a good agreement between parameters obtained in the fitting of the L^∞ and L^2 norms above is one such indication; another one is the agreement of the parameters a and b between examples of this subsection and the previous one. We also note the similarity of the blow-up profiles in Figs. 27 and 29 suggesting a universal blow-up profile $P(X, Y)$ which, however, we do not investigate it in this paper.

Acknowledgements CK and NS were partially supported by the ANR-FWF Project ANuI-ANR-17-CE40-0035, the isite BFC project NAANoD, the ANR-17-EURE-0002 EIPHI and by the European Union Horizon 2020 research and innovation program under the Marie Skłodowska-Curie RISE 2017 Grant Agreement No. 778010 IPaDEGAN. SR was partially supported by the NSF Grant DMS-1815873/1927258; she would also like to thank the AROOO ('A Room of Ones's Own') initiative for focused research time for this project.

References

- Arbunich, J., Klein, C., Sparber, C.: On a class of derivative Nonlinear Schrödinger-type equations in two spatial dimensions. *M2AN* **53**(5), 1477–1505 (2019)
- Côte, R., Muñoz, C., Pilod, D., Simpson, G.: Asymptotic stability of high-dimensional Zakharov–Kuznetsov solitons. *Arch. Ration. Mech. Anal.* **220**(2), 639–710 (2016)

- Cox, S., Matthews, P.: Exponential time differencing for stiff systems. *J. Comput. Phys.* **176**, 430–455 (2002)
- de Bouard, A.: Stability and instability of some nonlinear dispersive solitary waves in higher dimension. *Proc. R. Soc. Edinburgh Sect. A* **126**(1), 89–112 (1996)
- Faminskii, A.V.: The Cauchy problem for the Zakharov–Kuznetsov equation. (Russian) *Differentsialnye Uravneniya* **31**(6), 1070–1081 (1995), translation in *Differential Equations* **31**(6), 1002–1012 (1995)
- Farah, L.G., Linares, F., Pastor, A.: A note on the 2D generalized Zakharov–Kuznetsov equation: local, global, and scattering results. *J. Differ. Equ.* **253**, 2558–2571 (2012)
- Farah, L.G., Holmer, J., Roudenko, S.: Instability of solitons-revisited, II: the supercritical Zakharov–Kuznetsov equation. *Contemp. Math.*, 725, pp. 89–109. Amer. Math. Soc (2019)
- Farah, L.G., Holmer, J., Roudenko, S.: Instability of solitons in the 2D cubic Zakharov–Kuznetsov equation, Fields Institute Communications. In: Miller, P., Perry, P., Saut, J.C., Sulem, C. (eds.) *Nonlinear Dispersive Partial Differential Equations and Inverse Scattering*, vol. 83. Springer, New York (2019)
- Farah, L.G., Holmer, J., Roudenko, S., Yang, K.: Blow-up in finite or infinite time of the 2D cubic Zakharov–Kuznetsov equation. [arXiv:1810.05121](https://arxiv.org/abs/1810.05121) (2018)
- Hochbruck, M., Ostermann, A.: Exponential integrators. *Acta Numer.* (2010). <https://doi.org/10.1017/S0962492910000048>
- Kazeykina, A., Klein, C.: Numerical study of blow-up and stability of line solitons for the Novikov–Veselov equation. *Nonlinearity* **30**, 2566–2591 (2017)
- Kinoshita, S.: Global well-posedness for the Cauchy problem of the Zakharov–Kuznetsov equation in 2D. [arXiv:1905.01490](https://arxiv.org/abs/1905.01490) (2018)
- Klein, C.: Fourth order time-stepping for low dispersion Korteweg–de Vries and nonlinear Schrödinger equation. *ETNA* **29**, 116–135 (2008)
- Klein, C., Peter, R.: Numerical study of blow-up in solutions to generalized Kadomtsev–Petviashvili equations. *Discrete Continuous Dyn. Syst. Ser. B* **19**, 1689–1717 (2014)
- Klein, C., Peter, R.: Numerical study of blow-up in solutions to generalized Korteweg–de Vries equations. *Phys. D* **304**, 52–78 (2015)
- Klein, C., Roidot, K.: Fourth order time-stepping for Kadomtsev–Petviashvili and Davey–Stewartson equations. *SIAM J. Sci. Comput.* **33**(6), 3333–3356 (2011). <https://doi.org/10.1137/100816663>
- Klein, C., Stoilov, N.: A numerical study of blow-up mechanisms for Davey–Stewartson II systems. *Stud. Appl. Math.* (2018). <https://doi.org/10.1111/sapm.12214>
- Lagarias, J.C., Reeds, J.A., Wright, M.H., Wright, P.E.: Convergence properties of the Nelder–Mead simplex method in low dimensions. *SIAM J. Optim.* **9**(1), 112–147 (1998)
- Lannes, D., Linares, F., Saut, J.-C.: The Cauchy problem for the Euler–Poisson system and derivation of the Zakharov–Kuznetsov equation. *Prog. Nonlinear Differ. Equ. Appl.* **84**, 181–213 (2013)
- Linares, F., Pastor, A.: Well-posedness for the two-dimensional modified Zakharov–Kuznetsov equation. *SIAM J. Math. Anal.* **41**(4), 1323–1339 (2009)
- Martel, Y., Merle, F.: Blow up in finite time and dynamics of blow up solutions for the L^2 -critical generalized KdV equation. *J. Am. Math. Soc.* **15**, 617–664 (2002)
- Melkonian, S., Maslowe, S.A.: Two dimensional amplitude evolution equations for nonlinear dispersive waves on thin films. *Phys. D* **34**, 255–269 (1989)
- Merle, F.: Existence of blow-up solutions in the energy space for the critical generalized KdV equation. *J. Am. Math. Soc.* **14**(3), 555–578 (2001)
- Monro, S., Parkes, E.J.: The derivation of a modified Zakharov–Kuznetsov equation and the stability of its solutions. *J. Plasma Phys.* **62**(3), 305–317 (1999)
- Ribaud, F., Vento, S.: A note on the Cauchy problem for the 2D generalized Zakharov–Kuznetsov equations. *C. R. Math. Acad. Sci. Paris* **350**(9–10), 499–503 (2012)
- Saad, Y., Schultz, M.: GMRES: a generalized minimal residual algorithm for solving nonsymmetric linear systems. *SIAM J. Sci. Comput.* **7**, 856–869 (1986)
- Sipicic, R., Benney, D.J.: Lump Interactions and Collapse in the Modified Zakharov–Kuznetsov equation. *Stud. Appl. Math.* **105**(4), 385–403 (2000)
- Sulem, C., Sulem, P.-L.: *The Nonlinear Schrödinger Equation. Self-Focusing and Wave-Collapse*. Springer, Berlin (1999)
- Valet, F.: Asymptotic K-soliton-like solutions of the Zakharov–Kuznetsov type equations. [arXiv:2005.08518](https://arxiv.org/abs/2005.08518)
- Yang, K., Roudenko, S., Zhao, Y.: Blow-up dynamics in the mass super-critical NLS equations. *Phys. D* **396**, 47–69 (2019)

Zakharov, V.E., Kuznetsov, E.A.: On three dimensional solitons. Zhurnal Eksp. Teoret. Fiz **66**, 594–597 (1974). [in russian], Sov. Phys JETP **39**(2), 285–286 (1974)
Video Gallery <https://mathphys.fr/video/>

Publisher's Note Springer Nature remains neutral with regard to jurisdictional claims in published maps and institutional affiliations.